Epistatic interactions within the influenza virus polymerase complex mediate mutagen resistance and replication fidelity

Running Title: Mutagen resistance in influenza virus

Matthew D. Pauly[1], Daniel M. Lyons[2], and Adam S. Lauring[1,2,3] *

[1] Department of Microbiology and Immunology, University of Michigan, Ann Arbor, MI 48109

[2] Department of Ecology and Evolutionary Biology, University of Michigan, Ann Arbor, MI 48109

[3] Division of Infectious Diseases, Department of Internal Medicine, University of Michigan, Ann Arbor, MI 48109

* Corresponding author

Adam S. Lauring

1150 W. Medical Center Dr.

MSRB1 Room 5510B

Ann Arbor, MI 48109-5680

alauring@med.umich.edu

Abstract Word Count: 243 and 143

Main Text Word Count: 5,852

1   **Abstract**

2   Lethal mutagenesis is a broad-spectrum antiviral strategy that employs mutagenic nucleoside

3   analogs to exploit the high mutation rate and low mutational tolerance of many RNA viruses.

4   Studies of mutagen-resistant viruses have identified determinants of replicative fidelity and the

5   importance of mutation rate to viral population dynamics. We have previously demonstrated the

6   effective lethal mutagenesis of influenza virus using three nucleoside analogs as well as the

7   virus's high genetic barrier to mutagen resistance. Here, we investigate the mutagen-resistant

8   phenotypes of mutations that were enriched in drug-treated populations. We find that PB1

9   T123A has higher replicative fitness than the wild type, PR8, and maintains its level of genome

10   production during 5-fluorouracil treatment. Surprisingly, this mutagen-resistant variant also has

11   an increased baseline rate of C to U and G to A mutations. A second drug-selected mutation,

12   PA T97I, interacts epistatically with PB T123A to mediate high-level mutagen resistance,

13   predominantly by limiting the inhibitory effect of nucleosides on polymerase activity. Consistent

14   with the importance of epistatic interactions in the influenza polymerase, we find that nucleoside

15   analog resistance and replication fidelity are strain dependent. Two previously identified

16   ribavirin-resistance mutations, PB1 V43I and PB1 D27N, do not confer drug resistance in the

17   PR8 background, and the PR8-PB1 V43I polymerase exhibits a normal baseline mutation rate.

18   Our results highlight the genetic complexity of the influenza virus polymerase and demonstrate

19   that increased replicative capacity is a mechanism by which an RNA virus can counter the

20   negative effects of elevated mutation rates.

21

22   **Importance**

23   RNA viruses exist as genetically diverse populations. This standing genetic diversity gives them

24   the potential to adapt rapidly, evolve resistance to antiviral therapeutics, and evade immune

25   responses. Viral mutants with altered mutation rates or mutational tolerance have provided

26   insights into how genetic diversity arises and how it affects the behavior of RNA viruses. To this

27   end, we identified variants within the polymerase complex of influenza virus that are able

28   tolerate drug-mediated increases in viral mutation rates. We find that drug resistance is highly

29   dependent on interactions among mutations in the polymerase complex. In contrast to other

30   viruses, influenza virus counters the effect of higher mutation rates primarily by maintaining high

31   levels of genome replication. These findings suggest the importance of maintaining large

32   population sizes for viruses with high mutation rates and show that multiple proteins can affect

33   both mutation rate and genome synthesis.

34

35   Key Words – influenza virus, mutation rate, lethal mutagenesis, fidelity, polymerase, evolution

36

37   **Introduction**

38   Influenza virus remains a persistent health threat due to its rapid rate of evolution (1). This rapid

39   rate of evolution is attributable, in part, to the virus' very high mutation rate (2-5). Influenza virus

40   rapidly acquires antigenic changes and antiviral resistance, which limit the effectiveness of

41   vaccines and antiviral drugs (6, 7). As in many RNA viruses, influenza virus' low fidelity is due to

42   the absence of proofreading and repair mechanisms during genome replication (8-10). We have

43   previously estimated influenza's mutation rate to be greater than 1×10^{-4} mutations per

44   nucleotide per RNA strand replicated, which suggests that approximately 2 new mutations are

45   introduced into every newly synthesized genome (11). As a result, influenza viruses exist as

46   swarms of distinct genetic variants, which provide a rich substrate for natural selection of

47   adaptive mutations.

48

49   While some mutations are beneficial to a virus, the vast majority of mutations are detrimental

50   (12). In influenza virus, we have found that 30% of single nucleotide changes are lethal and

51   70% decrease replicative fitness (13). Lethal mutagenesis is an antiviral strategy that utilizes

52   nucleoside analogues to increase a virus' mutation rate and the frequency of deleterious or

2

53   lethal mutations (14, 15). The effectiveness of lethal mutagenesis has been demonstrated in

54   many viral systems, including poliovirus, human immunodeficiency virus, foot-and-mouth

55   disease virus (FMDV), lymphocytic choriomeningitis virus, and influenza virus (16-22). A

56   hallmark of lethal mutagenesis is a reduction in viral specific infectivity due to the increased

57   genesis of genomes that do not encode a functional complement of viral proteins. In addition to

58   their mutagenic effects, many nucleoside analogs also inhibit the activity of viral RNA-

59   dependent RNA-polymerases (RdRp) (23-26).

60

61   While initially thought to be a resistance-proof strategy, RNA virus mutants that are resistant to

62   lethal mutagenesis have been identified by serial passage of viral populations in low

63   concentrations of drug (20, 27-32). In most cases, mutagen resistant variants encode

64   polymerases that exhibit increased replication fidelity, and characterization of these mutants has

65   elucidated the molecular mechanisms governing mutation rate. With a lower baseline mutation

66   rate, these variants require higher concentrations of mutagenic drug to increase the viral

67   mutation rate to the same level as a wild type virus.

68

69   Other mechanisms of nucleoside resistance have been reported for RNA viruses. Polymerase

70   mutants in FMDV mediate resistance by selecting against nucleoside misincorporation, possibly

71   biasing the virus' mutation spectrum (33, 34). Interestingly, a mutation in the polymerase

72   associated 2C protein of FMDV also appears to alter mutagen-induced mutational bias (35).

73   The DNA bacteriophage ΦX174 mitigates the impact of mutagenesis by delaying lysis and

74   increasing its burst size, a mechanism of genetic robustness that paradoxically maintains

75   unmutagenized progeny (36, 37). Finally, a virus' primary sequence also affects mutagen

76   sensitivity through its genetic robustness, or ability to buffer the fitness effects of mutations (38,

77   39). Collectively, these works have elucidated how mutation rate and mutational tolerance

78   shape the diversity and structure of RNA virus populations.

3

79

80   Current models of lethal mutagenesis and mutagen resistance are derived almost entirely from

81   studies of positive sense RNA viruses. In contrast to this large group of viruses, influenza virus

82   replicates its genome using a heterotrimeric replicase complex. This complex consists of the

83   PB2, PA, and PB1 proteins, which have 5'-cap binding, 5'-cap stealing, and RdRp activities,

84   respectively (40). The constraints of this polymerase complex may alter the genetic barrier to

85   mutagen resistance or its potential mechanisms. Two polymerase variants with reduced

86   sensitivity to the mutagen ribavirin have been reported for influenza virus. The PB1 V43I

87   mutation was identified as a minority variant upon serial passage of A/Wuhan/35/95 in low

88   concentrations of ribavirin and appears to have altered fidelity in that genetic background (20). A

89   second mutation, PB1 D27N, was recovered in a screen for PB1 mutants in WSN33 that

90   maintained RNA synthesis during ribavirin treatment (41, 42).

91

92   We previously demonstrated the mutagenic activity of ribavirin, 5-azacytidine, and 5-fluorouracil

93   in influenza virus (21). Interestingly, serial passage of influenza virus populations in sublethal

94   concentrations of each of these three drugs did not lead to population-wide resistance. We did,

95   however, identify three mutations – PB1 T123A, PB1 M645I, and PA T97I – that were enriched

96   in replicate drug-selected populations (21). Here, we characterize the effects of these three

97   mutations on nucleoside analog sensitivity, viral fitness, and replicative fidelity. Additionally, we

98   characterize the previously identified PB1 V43I and PB1 D27N mutants in the PR8 genetic

99   background. We show that mutagen resistant variants in the influenza polymerase complex

100   have similar fidelity to wild type viruses. In contrast to what has been found in other viral

101   systems, these variants mediate resistance by limiting the mutagenic and polymerase-inhibitory

102   effects of nucleoside drugs.

103

104   **Results**

4

105   We have previously shown that serial passage of influenza A PR8 in low concentrations of

106   ribavirin, 5-fluorouracil, or 5-azacytidine does not select for population-wide resistance over 16

107   passages (21). This result did not preclude the possibility that there were resistance mutations

108   present at a low level within these populations or that their phenotypic effect was masked by the

109   impact of mutations elsewhere in the genome. Consistent with this hypothesis, next generation

110   sequencing revealed a number of mutations that were shared among drug-passaged

111   populations and that did not achieve fixation (21). We identified candidate resistance mutations

112   in the PB2, PB1, and PA open reading frames based on their presence in mutagen-passaged

113   viral populations and absence in either the starting population or control populations passaged

114   without drug treatment. Three nonsynonymous mutations met these criteria. The PB1 T123A

115   mutation was found in all three 5-fluorouracil (5FU) populations at frequencies of 34%, 31%,

116   and 8%. The PA T97I mutation was found in all three ribavirin-passaged populations at

117   frequencies of 88%, 55%, and 11%. We also identified the PB1 M645I mutation at frequencies

118   of 90%, 14%, and 1% in these same ribavirin-passaged populations. The ribavirin resistant

119   mutant, PB1 V43I, was not found in any of the populations, and PB1 D27N was only found in

120   one ribavirin-passaged population at a frequency of 3%. We introduced each of these five

121   mutations into a clean PR8 genetic background. We also generated the double mutants PB1

122   T123A ; PA T97I and PB1 M645I ; PA T97I. The PB1 M645I ; PA T97I double mutant was

123   identified in our ribavirin passaged viral populations. The PB1 T123A ; PA T97I double mutant

124   was not found naturally, but these mutations on distinct segments could plausibly interact

125   genetically.

126

127   *Mutagen sensitivity*

128   Given their enrichment in drug-passaged populations, we hypothesized that one or more of the

129   mutations in the polymerase complex would mediate mutagen resistance. We tested each of the

130   variant polymerases for reduced nucleoside sensitivity by comparing titers after replication of

131   the corresponding virus populations in mock- or drug-treated cell cultures 24 hours post

132   infection (Figure 1). We selected drug concentrations that would decrease infectious viral titers

133   by 3-4 orders of magnitude so that we could observe a range of resistance phenotypes, while

134   limiting cytotoxicity. The concentrations used – 20µM ribavirin, 20µM 5-azacytidine, and 100µM

135   5FU – were roughly 3 times higher than those in which our mutants were selected (21).

136

137   The PB1 T123A mutation, which was identified in 5FU passaged populations, conferred a 6-fold

138   reduction in sensitivity to 100µM 5FU (Dunnett's adjusted p-value = 0.007), but no change in

139   sensitivity to 20µM ribavirin or 20µM 5-azacytidine. Interestingly, PA T97I, which was identified

140   only in populations passaged in ribavirin, conferred resistance to 100µM 5FU (6-fold sensitivity

141   reduction, Dunnett's adjusted p-value = 0.011), but not to 20µM ribavirin or 20µM 5-azacytidine.

142   The other mutation enriched in ribavirin-passaged populations, PB1 M645I, did not alter

143   sensitivity to any of the three nucleoside analogs. We found that the two previously identified

144   ribavirin resistant mutants, PB1 D27N and PB1 V43I, were just as sensitive as the wild type

145   PR8 strain to both ribavirin and 5FU. The PB1 D27N mutant appeared to be more sensitive than

146   WT PR8 to 5-azacytidine (13-fold increase, Dunnett's adjusted p-value < 0.0001). These data

147   suggest that the resistance phenotypes of PB1 D27N and PB1 V43I are dependent on strain

148   background. Of the five single mutants tested, only PB1 T123A and PA T97I exhibited reduced

149   sensitivity to our panel of nucleoside analogs.

150

151   The PB1 M645I and PA T97I double mutant, which was identified in ribavirin-passaged

152   populations, exhibited a pattern of nucleoside analog sensitivity that was very similar to the PA

153   T97I single mutant (5-fold reduction in sensitivity to 5FU, Dunnett's adjusted p-value = 0.018).

154   Surprisingly, the PB1 T123A ; PA T97I double mutant, which was not found in passaged

155   populations, exhibited a 93-fold reduction in sensitivity to 100µM 5FU (Dunnett's adjusted p-

156   value < 0.0001) and a slight, but statistically significant reduction in sensitivity to 20µM ribavirin

6

157 (6-fold reduction, Dunnett's adjusted p-value = 0.034). Paradoxically, this double mutant was

158 more sensitive to treatment with 20µM 5-azacytidine than WT PR8 (8-fold increase, Dunnett's

159 adjusted p-value = 0.0004). Thus, these two mutations were synergistic with respect to 5FU

160 resistance while at the same time increasing 5-azacytidine sensitivity.

161

162 *Replicative fitness*

163 Mutagen resistant variants often have a fitness defect compared to their wild type counterparts.

164 We used a serial passage competition assay to measure the replicative fitness of each mutant

165 virus relative to the WT PR8 and performed growth curves to quantify RNA genome production.

166 In the absence of mutagenic drug, we identified a range of fitness effects among the

167 polymerase mutants (Figure 2A). The PB1 T123A virus was more fit than WT, even out of drug,

168 and produced more genomes early in replication than either WT or the other mutants (Figure

169 2B). Both PB1 M645I and PA T97I were essentially neutral. The PB1 T123A ; PA T97I double

170 mutant, which was highly resistant to 5FU, exhibited reciprocal sign epistasis, as it had a

171 marked decrease in fitness while each single mutant was beneficial or neutral. Consistent with

172 the lower fitness of this mutant, it produced fewer genomes than the wild type (Figure 2B). The

173 PB1 M645I ; PA T97I double mutant had higher fitness than WT, suggesting that selection of

174 PB1 M645I in ribavirin-passaged populations reflected culture-adaptation rather than mutagen

175 resistance. Both PB1 D27N and PB1 V43I had dramatically reduced fitness compared with WT.

176 The decreased fitness of PB1 V43I is consistent with previous data on its growth kinetics (20).

177 As PB1 M645I, PB1 D27N, and the PB1 M645I ; PA T97I double mutant were not resistant to

178 any of the nucleoside drugs, we did not analyze them further.

179

180 We measured the fitness of PB1 T123A, PA T97I, and the double mutant PB1 T123A ; PA T97I

181 in the presence of 25µM and 50µM 5FU to better quantify their mutagen sensitivity. We used

182 lower concentrations of drug in this serial passage experiment to avoid population extinction

183   (see 100µM Figure 1 and (21)). We found that the relative fitness of all three 5FU resistant

184   variants increased significantly when competed in drug, but that the double mutant only

185   competed effectively with WT at the highest drug concentrations (Figure 2C). These data

186   indicate that the three mutant viruses have varying resistance to 5-fluorouracil. The range of

187   fitness values that we observed suggests that each has a different mechanism of resistance.

188

189   *Mutation rate*

190   The most commonly identified mechanism of mutagen resistance in RNA viruses is altered

191   baseline polymerase fidelity. We determined the baseline mutation rate of our three 5FU

192   resistant variants using a Luria-Delbrück fluctuation test that can measure the rates of all 12

193   mutational classes ((11) and Figure 3). We also evaluated PB1 V43I, which has been reported

194   to be a fidelity variant (20, 43). We used this novel fluctuation test to interrogate four of the most

195   common mutational classes (A to G, C to U, G to A, and U to C), for which the assay has the

196   greatest discriminatory power. These same mutational classes are also those most affected by

197   5FU treatment. Both PA T97I and the PB1 T123A ; PA T97I double mutant had mutation rates

198   that were very similar to those of WT. Unexpectedly, PB1 T123A made significantly more C to U

199   and G to A mutations than WT. While we cannot rule out differences in the rates of transversion

200   mutations, these less common mutation classes would be unlikely to affect overall polymerase

201   fidelity. The PB1 V43I mutant had no evident resistance to nucleoside analogs or altered

202   mutation rate in the PR8 genetic background. As the fidelity and resistance phenotypes of this

203   mutation were demonstrated in the A/Wuhan/359/95 H3N2 strain, we suggest that its effects are

204   modulated by epistatic interactions within the PR8 polymerase complex.

205

206   We next assessed the impact of drug treatment on the mutation rates of these polymerase

207   mutants. We used 15µM 5FU because the larger titer reductions with higher drug

208   concentrations preclude precise measurements of mutation rates in our fluctuation test. Again,

209   we measured the rates of the four transition mutation classes impacted by 5FU (Figure 4). The

210   increase in transition mutations in the PA T97I mutant with 5FU treatment was similar to that of

211   WT. In contrast, the PB1 T123A mutant, which has an increased baseline rate of C to U and G

212   to A mutations, selectively buffers against further drug-induced increases in these same classes.

213   This phenotype is most pronounced for C to U mutations. While 15µM 5FU increased all

214   transition mutations approximately 5-fold in PR8, we observed almost no change in C to U

215   mutations in the PB1 T123A mutant. The PB1 T123A ; PA T97I double mutant also buffers

216   against C to U mutations induced by 5FU, albeit not as dramatically as the PB1 T123A single

217   mutant. Together, these data show that PB1 T123A has an increased rate for two transition

218   mutation types while also limiting further induction by 5FU treatment.

219

220   *Genome infectivity*

221   Increases in viral mutation rates are often accompanied by decreases in the specific infectivity

222   of the population. Accordingly, a virus resistant to the mutagenic effects of a nucleoside analog

223   would be expected to exhibit a smaller decrease in specific infectivity upon drug treatment. We

224   measured the effect of 100µM 5FU on the specific infectivity of the three resistant mutants by

225   measuring the number of infectious particles per genome (Figure 5). Drug treatment reduced

226   the specific infectivity of all three mutants, consistent with the drug's mutagenic effects. In all

227   cases, the magnitude of the effect was similar to that of treated WT viruses. These data indicate

228   that the observed decrease in 5FU-induced C to U mutations in PB1 T123A virus is not

229   sufficient to cause a corresponding change in specific infectivity. The observed decreases in

230   specific infectivity in 5FU are more likely due to the more common A to G and U to C mutation

231   classes. Therefore, the limited fidelity phenotype of PB1 T123 is unlikely to contribute

232   significantly to the virus' mutagen resistance.

233

234   *Genome production*

9

235   Given that the resistance phenotype of our three polymerase variants was not due to altered

236   fidelity, we evaluated their ability to resist 5FU-mediated inhibition of genome synthesis. We

237   assessed the kinetics of genome replication in the presence and absence of 100μM 5FU by

238   measuring the number of genomes in the supernatants of cells infected with each viral mutant.

239   Treatment with 5FU caused a 10- to 100-fold decrease in genome copies generated by WT

240   relative to controls (Figure 6). The PA T97I mutant exhibited a similar decrease in genome

241   output in drug. In contrast, we observed smaller decreases in genome production in drug for

242   both PB1 T123A and PB1 T123A ; PA T97I, especially at later time points. At 24 hours post

243   infection, there was no significant difference on the number of genomes for PB1 T123A. The

244   PB1 T123A ; PA T97I double mutant maintained its generally lower level of genome production

245   across multiple time points, consistent with epistatic interactions between these mutations and

246   their impact on 5FU resistance.

247

248   **Discussion**

249   Mutagen resistant variants have been a valuable tool for probing the determinants of RNA virus

250   mutation rates and the effect of mutation rate on viral population diversity (9, 10, 20, 27-30). We

251   therefore investigated the mechanisms through which influenza virus can resist the antiviral

252   effects of nucleoside analog drugs. We identified PB1 T123A and PA T97I as two 5-fluorouracil

253   resistance mutations that interact epistatically. We also found evidence for epistasis in the

254   previously identified ribavirin resistance mutants, PB1 D27N and PB1 V43I, as they remain

255   sensitive to drug in the PR8 genetic background. The three mutagen-resistant viruses reported

256   here are not high fidelity variants and the PB1 T123A variant paradoxically exhibits a higher

257   baseline mutation rate for certain mutational classes. We identified increased genome output as

258   the main mechanism of 5-fluroruracil resistance for PB1 T123A and resistance to drug-mediated

259   RdRp inhibition as the mechanism for the PB1 T123A ; PA T97I double mutant.

260

261   While the literature on lethal mutagenesis and fidelity variants has largely focused on viruses

262   with a monomeric RdRp, the influenza replicase complex is composed of three proteins; PB1,

263   PB2, and PA (44-46). The PB1 protein is the RdRp, which is shaped like a right hand with the

264   fingers and thumb domains enclosing the palm-based active site. Mutations that alter the fidelity

265   of RNA virus replication have rarely been observed within the active site of the RdRp (47-49).

266   The PB1 T123 mutation is located within the fingers domain near where the RNA template

267   enters the RdRp active site, while PA T97 is located far from the RdRp active site in the

268   endonuclease domain of this PB1-associated protein. We suggest that the nature of the

269   influenza polymerase complex allows for an array of intergenic, and possibly intragenic,

270   epistatic interactions that mediate both replication fidelity and mutagen resistance.

271

272   We identified PB1 T123A as a mutation that mediates resistance to 5FU, but not ribavirin or 5-

273   azacytidine. While mutagen selection has been used to identify high fidelity variants in a number

274   of viral systems, the PB1 T123A virus actually has a marginally elevated mutation rate. This

275   reduced fidelity is class-specific with the largest increase in C to U transitions. Despite its higher

276   mutation rate, this virus had higher replicative fitness than WT and produced more genomes in

277   the early stages of replication. We also found that while the baseline C to U mutation rate is

278   higher for this mutant, the mutagenic effect of 5FU on this mutational class is dramatically

279   reduced. This phenotype is similar to that of the ribavirin resistant FMDV mutant, 3D M296I (32,

280   50) and may reflect increased selectivity against misincorporation of 5FU. Our finding of

281   reduced mutagenesis, however, seems inconsistent with the specific infectivity decrease we

282   observe upon drug treatment. This may indicate that 5FU-mediated increases in the two most

283   common mutation classes (A to G and U to C) are the main contributor to the observed

284   decrease in specific infectivity with drug treatment. The most likely mechanism of resistance

285   appears to be through its increase in replicative fitness in the absence of drug (Figure 2).

286   Importantly, the mutant also maintained its genomic output in the presence of 5FU, a phenotype

287   augmented by PA T97I (Figure 6, see below). The fact that PB1 T123A did not counter the

288   detrimental effect of ribavirin and 5-azacytidine suggest that the resistance phenotype mediated

289   by PB1 T123A is not broadly applicable to other nucleoside analogs.

290

291   The other mutation we investigated was located in the PB1 associated protein, PA. This mutant,

292   PA T97I, exhibited fitness and genome production phenotypes that were very similar to those of

293   the wild type. Interestingly, this mutant was selected during ribavirin treatment but was resistant

294   to 5FU and not ribavirin. This mutant closely mirrored PB1 T123A in terms of its smaller

295   decreases in infectious titer upon treatment with 5FU. Unlike PB1 T123A, the baseline and 5FU-

296   induced mutation rates of PA T97I are similar to those of the wild type virus for all transition

297   mutation classes. This mutant also exhibited decreases in genome production during 5FU

298   treatment that were similar to those of WT. It is currently unclear how PA T97I mediates its

299   resistance to 5FU. Since its resistance was more pronounced at higher concentrations of 5FU, it

300   is possible that the technical limitations in the amount of 5FU we could use for accurate

301   mutation rate measurements prevented us from observing a subtle phenotype.

302

303   Even though PB1 T123A and PA T97I evolved in different passage cultures, we combined them

304   to make a double mutant. Serendipitously, we found that this double mutant exhibited the most

305   dramatic 5FU resistance phenotype of any of the mutants we tested. These two mutations led to

306   a reduced fitness phenotype characteristic of reciprocal sign epistasis; the combination of a

307   mutant with increased fitness (PB1 T123A) with a neutral mutant (PA T97I) led to a double

308   mutant with very low fitness and significantly reduced genomic RNA output. At the

309   concentrations of 5FU used for selection of resistant variants, this double mutant has a fitness

310   lower than wild type, even though it is highly resistant to the drug. This finding likely explains

311   why it did not arise within our experimentally evolved populations. The double mutant virus had

312   a nearly identical spectrum of transition mutation rates to the wild type virus and only slightly

313   mitigated the mutagenic effect of 5FU on C to U mutations. Drug resistance seems to be driven

314   primarily by maintaining high genomic output during 5FU treatment, an effect that appears to be

315   more pronounced compared to the PB1 T123A single mutant (Figure 6). Treatment with

316   nucleoside analog led to almost no reduction in the number of genome segments that are

317   released from infected cells. This mechanism allows for more infectious viral particles to be

318   produced than wild type despite similar levels of mutagenesis and specific infectivity decreases.

319

320   Our examination of two other mutagen-resistant variants further suggests the importance of

321   epistatic interactions within the influenza polymerase complex. Previously, PB1 D27N was

322   identified as a mutation that limited ribavirin inhibition of RNA synthesis in a replicon system (41,

323   42). We find that this mutant is not resistant to ribavirin or other mutagenic nucleoside analogs

324   in a replication competent PR8 virus. Additionally, we found that the mutagen resistance and

325   fidelity phenotype of PB1 V43I is strain dependent. This mutation, which mediates ribavirin

326   resistance in the A/Wuhan/359/95 H3N2 and A/Vietnam/1203/04 H5N1 strains, is sensitive to

327   drug in the PR8 genetic background (20). The PB1 V43I mutant, which has been suggested to

328   be a fidelity variant even in the PR8 background (43), shows no difference in the rate of

329   transition mutations in PR8. These findings suggest that there are likely to be epistatic

330   interactions governing polymerase activity and fidelity in influenza virus, and that the ability of

331   one virus to evolve resistance to a mutagen may not be reflective of how another strain evolves

332   in the face of the same selective pressure.

333

334   While the field has often focused on the mutagenic effects of nucleoside drugs, our results

335   suggest that their effect on viral replicative capacity may be more important in influenza virus.

336   Both PB1 T123A and PB1 T123A ; PA T97I are able to effectively maintain their titers in drug by

337   limiting the impact of 5FU on genome production. We have previously shown that the decreases

338   in specific infectivity associated with nucleoside analog treatment (up to 10-fold) are much less

13

339 than the effect of these compounds on infectious titer output (> 1,000-fold) (21). The

340 identification of resistant variants that maintain genome output with little impact on specific

341 infectivity suggest that inhibition of RdRp activity is the main mechanism of action for 5FU. As

342 we did not identify mutations that mediate ribavirin or 5-azacytidine resistance, we cannot say

343 whether mutagenic or non-mutagenic mechanisms are dominant for these drugs.

344

345 Finally, we show that polymerases with increased replicative capacity can counteract the

346 mutagenic effects of nucleoside drugs. This is a less recognized mechanism of mutational

347 robustness, but one that is entirely consistent with population genetic theory (37, 51). The

348 efficiency of negative selection is the product of the effective population size and the average

349 mutational fitness effect. Increased genome production will lead to larger populations, and

350 strong selection will quickly purge the large numbers of mutants with lower fitness, leaving the

351 most fit sequence to dominate the mutant spectrum. This "safety in numbers" phenomenon

352 leads to population-level mutational robustness even in the setting of individual-level

353 hypersensitivity. Therefore, studies of mutagen resistance continue to provide new insights into

354 the biochemistry of RNA virus replication and fundamental aspects of their population genetics.

355

356 **Materials and Methods**

357 *Cells, viruses, plasmids, and drugs*

358 Human embryonic kidney 293T fibroblasts were provided by Dr. Raul Andino (University of

359 California San Francisco). Madin Darby canine kidney (MDCK) cells were provided by Dr.

360 Arnold Monto (University of Michigan). Both cell lines were maintained in growth medium

361 (Dulbecco's modified Eagle medium (Gibco 11965) supplemented with 10% fetal bovine serum

362 and 25 mM HEPES) at 37°C and 5% CO_2 in a humidified incubator.

363

14

364   MDCK cells expressing the hemagglutinin (HA) protein of influenza A/Puerto Rico/8/1934 H1N1

365   (MDCK-HA cells) were generated by co-transfection with a pCABSD plasmid that expresses a

366   Blasticidin S resistance gene and a pCAGGS plasmid encoding the influenza A/Puerto

367   Rico/8/1934 H1N1 HA gene (52, 53). Cells stably expressing HA were selected in growth

368   medium containing 5µg/mL Blasticidin S and were enriched for high HA expression by staining

369   with an anti-HA antibody (1:1000 dilution, Takara c179) and an Alexa 488-conjugated anti-

370   mouse IgG (1:200 dilution, Life Technologies A11001) followed by fluorescence-activated cell

371   sorting on a FACSAria II (BD Biosciences). Over the course of 5 passages, cells were sorted

372   three times to achieve a final population in which >99% of cells were positive for high level HA

373   expression.

374

375   All eight genomic segments of influenza A/Puerto Rico/8/1934 H1N1 (PR8) (ATCC VR-1469)

376   were cloned into the pHW2000 vector (54). Briefly, genomic RNA was harvested from the

377   supernatants of infected cells using TRIzol reagent (Life Technologies 15596). Complementary

378   DNA was synthesized by reverse transcription PCR using SuperScript III (Invitrogen 18080051)

379   and Phusion high fidelity DNA polymerase (New England Biosciences M0530) with primers

380   described by Hoffmann and colleagues (55). PCR products and pHW2000 were digested using

381   BsmB1 (New England Biosciences R0580), Bsa1 (New England Biosciences R0535) or Aar1

382   (Thermo Scientific ER1581). Digested DNA was gel purified (Thermo Scientific K0691) and

383   PCR products were ligated into pHW2000 using T4 DNA ligase (New England Biosciences

384   M0202).

385

386   Mutant PB1 and PA segments were generated in the pHW2000 vector backbone using overlap

387   extension PCR (56). Two rounds of PCR were performed using Phusion high fidelity DNA

388   polymerase with pHW2000 plasmids encoding either PB1 or PA from the PR8 virus as a

389   template, the inner mutagenic primers (PB1 D27N, Fwd 5'-

15

390   CCCTTATACTGGAAACCCTCCTTACAGC-3', Rev 5'-

391   GCTGTAAGGAGGGTTTCCAGTATAAGGG-3'; PB1 V43I, Fwd 5'-

392   CACCATGGATACTATCAACAGGACAC-3', Rev 5'- GTGTCCTGTTGATAGTATCCATGGTG-3';

393   PB1 T123A, Fwd 5'- GTAGACAAGCTGGCACAAGGCCGAC-3', Rev 5'-

394   GTCGGCCTTGTGCCAGCTTGTCTAC-3'; PB1 M645I, Fwd 5'-

395   CAATGCAGTGATAATGCCAGCACATGG-3', Rev 5'-

396   CCATGTGCTGGCATTATCACTGCATTG-3'; PA T97I, Fwd 5'-

397   CAGTATTTGCAACATTACAGGGGCTGAG-3', Rev 5'-

398   CTCAGCCCCTGTAATGTTGCAAATACTG-3') and the outer primers containing AarI or BsmBI

399   restriction sites (PB1, Fwd 5'- TATTCACCTGCCTCAGGGAGCGAAAGCAGGCA-3', Rev 5'-

400   ATATCACCTGCCTCGTATTAGTAGAAACAAGGCATTT-3'; PA Fwd 5'-

401   TATTCGTCTCAGGGAGCGAAAGCAGGTAC-3', Rev 5'-

402   ATATCGTCTCGTATTAGTAGAAACAAGGTACTT-3'). Two first round PCR reactions using Fwd

403   inner primers with Rev outer primers and Rev inner primers with Fwd outer primers were

404   performed. The products of these reactions were purified using a GeneJET PCR Purification Kit

405   (Thermo K0701), mixed, and used as templates for a second-round PCR reaction using only the

406   outer primers. Full-length PB1 and PA genes were gel purified, digested, and cloned into

407   pHW2000 plasmid as above. PB1 containing a neutral genetic barcode was created in the same

408   manner using the inner mutagenic primers; 5'-

409   GATCACAACTCATTTCCAACGGAAACGGAGGGTGAGAGACAAT-3' and 5'-

410   ATTGTCTCTCACCCTCCGTTTCCGTTGGAAATGAGTTGTGATC-3'.

411

412   A pPOLI vector encoding enhanced green fluorescent protein (eGFP) with influenza HA

413   packaging sequences (ΔHA-GFP) was kindly provided by Luis Martinez-Sobrido (University of

414   Rochester). This construct contains eGFP flanked by the 78 3'-terminal bases (33 noncoding,

415   45 coding) and 125 5'-terminal bases (80 coding, 45 noncoding) of the influenza A/WSN/33

16

416   H1N1 HA segment, and lacks the HA translation initiation codon (57). QuikChange II site-

417   directed mutagenesis (Agilent Technologies 200523) was used to generate twelve mutant ΔHA-

418   GFP constructs with primers 5'- CTCGTGACCACCCTG<mutant

419   sequence>GTGCAGTGCTTCAGC-3' and 5'- GCTGAAGCACTGCAC<mutant

420   sequence'>CAGGGTGGTCACGAG-3', where mutant sequence corresponds to the sequences

421   ACCTACGAC for A to G mutation rate assessment, ACCCACGGC for C to U mutation rate

422   assessment, ACCTGCGGC for G to A mutation rate assessment, and ATATACGGC for U to C

423   mutation rate assessment and mutant sequence' is its reverse complement.

424

425   Viruses were rescued from plasmid transfections of MDCK and 293T co-cultures. pHW2000

426   plasmids encoding all eight influenza genome segments were mixed (500ng each) in Opti-MEM

427   (Gibco 31985062) with 8 µL of TransIT-LT1 (Mirus 2300) and incubated at room temperature for

428   30 minutes. Mixtures were added to 12-well plates seeded the previous day with 2 x 10^5 293T

429   cells and 1 x 10^5 MDCK cells and containing viral medium (Dulbecco's modified Eagle medium

430   (Gibco 11965) supplemented with 0.187% BSA, 25 mM HEPES, and 2 µg/mL TPCK treated

431   trypsin (Worthington Biochemical 3740)). The media was changed at 24 hours, and cell free

432   supernatants were harvested with the addition of 0.5% glycerol at 48 hours post transfection. All

433   rescued viruses were subsequently passaged on MDCK cells at an MOI of 0.01. Passage 1

434   (P1) virus was harvested at 48 hours post infection. All experiments used P1 virus stocks.

435

436   Ribavirin (1-[(2R,3R,4S,5R)-3,4-dihydroxy-5-(hydroxymethyl)oxolan-2-yl]-1H-1,2,4-triazole-3-

437   carboxamide) (Sigma-Aldrich R9644) was dissolved in phosphate buffered saline (PBS) at

438   100mM. 5-Fluorouracil (2,4-Dihydroxy-5-fluoropyrimidine) (Sigma-Aldrich F6627) was dissolved

439   in dimethyl sulfoxide (DMSO) at 384mM. 5-Azacytidine (4-Amino-1-(β-D-ribofuranosyl)-1,3,5-

440   triazin-2(1H)-one) (Sigma-Aldrich A2385) was dissolved in DMSO to make a stock at 100mM.

441   Aliquots of these drug stocks were stored at minus 20°C.

17

442

443 *Mutagen sensitivity assay*

444 Viral medium containing ribavirin, 5-azacytidine, or 5-fluorouracil was added to 24-well plates

445 that had been seeded with 6.5 x 10^4 MDCK cells the previous day. After three hours of drug

446 treatment, cells were infected with 1.5 x 10^4 pfu of virus (MOI 0.1) in 300 μl of viral media

447 containing drug. After one hour, the inoculum was removed and 500 μl of viral medium

448 containing drug was added. Twenty-four hours after infection, cell free supernatants were

449 harvested by adding 0.5% glycerol, centrifuging for 5 minutes at 3,000 x g, and freezing at -

450 80°C. Infectious viral titers were measured by $TCID_{50}$ assay with all wells scored for cytopathic

451 effect (CPE) at 4 days (58).

452

453 *Competition assay*

454 Mutant PB1 or PA viruses were mixed with PR8 viruses containing a neutral genetic barcode at

455 equivalent $TCID_{50}$ titers. Viral mixtures were used to infect 4 x 10^5 MDCK cells in a 12-well plate

456 at an MOI of 0.01. After 24 hours, supernatants were harvested and passaged 3 more times on

457 MDCK cells at an MOI of 0.01. All competitions were performed with three biological replicates.

458 Viral RNA was harvested from the supernatants of all passages using a Purelink Pro 96 viral

459 DNA/RNA kit (Invitrogen 12280). Superscript III and random hexamers were used to generate

460 cDNA. Quantitative PCR was used to determine the relative amount of total PB1 (primers 5'-

461 CAGAAAGGGGAAGATGGACA-3' and 5'-GTCCACTCGTGTTTGCTGAA-3'), barcoded PB1

462 (primers 5'-ATTTCCAACGGAAACGGAGGG-3' and 5'-AAACCCCCTTATTTGCATCC-3'), and

463 non-barcoded PB1 (primers 5'-ATTTCCAACGGAAACGGAGGG-3' and 5'-

464 AAACCCCCTTATTTGCATCC-3') in each sample. The quantities of barcoded and non-

465 barcoded PB1 genome segments at each passage were normalized by subtracting the Ct

466 threshold for the total PB1 primer set ($\Delta Ct = Ct_{competitior} - Ct_{total\ PB1}$). A relative ΔCt was obtained

467 by comparing these values at each passage to the initial P0 viral mixture ($\Delta\Delta Ct = \Delta Ct_{P1} - \Delta Ct_{P0}$).

18

468 The relative ΔCt was converted to the fold change in genome copies ($\Delta\text{ratio} = 2^{-\Delta\Delta Ct}$). The slope

469 of the differences between the $\log_{10}$ Δratios of the two viruses as a function of the passage

470 number is equal to the $\log_{10}$ relative fitness of the non-barcoded virus ($[\log_{10}\Delta\text{ratio}_{\text{non-barcoded}} - \log_{10}$

471 $\Delta\text{ratio}_{\text{barcoded}}]$/passage) (13).

472

473 *Specific infectivity assay*

474 RNA was extracted from the supernatants of virally infected cells using either TRIzol Reagent

475 (Life Technologies 15596), or Purelink Pro 96 Viral RNA/DNA Kit (Invitrogen 12280).

476 SuperScript III (Invitrogen 18080) was used to synthesize cDNA using random hexamers.

477 Quantitative PCR was performed on a 7500 Fast Real Time PCR system (Applied Biosystems).

478 Superscript III RT/Platinum Taq (Thermo 2574030) was used with the primers 5'-

479 GACCRATCCTGTCACCTCTGAC-3' and 5'-AGGGCATTYTGGACAAAKCGTCTA

480 -3', and the TaqMan probe FAM-TGCAGTCCTCGCTCACTGGGCACG-3' with Blackhole

481 Quencher 1 with an annealing temperature of 55°C for M segment copy number measurement.

482 Quantification of cDNA copy number based on cycle threshold (Ct) values was performed using

483 standard curves from ten-fold dilutions of plasmid containing the M gene of A/Puerto

484 Rico/8/1934 H1N1. The ratio of the infectious titer per mL to the genome copy number per mL is

485 the specific infectivity of the sample.

486

487 *Mutation rate assay*

488 Twenty-four wells containing 1.2×10^4 MDCK-HA cells were infected with 400 TCID$_{50}$ of

489 influenza viruses encoding mutant ΔHA-GFP segments in viral medium. Supernatants were

490 transferred to black 96-well plates (Perkin Elmer 6005182) containing 1.5×10^4 MDCK cells and

491 50μL of viral media at 17-23 hours post infection, depending on the mutation class and drug

492 treatment. Two wells were infected with virus equivalent to the amount used to initially infect the

493 parallel cultures. These wells were used to determine N_i (initial population size) in the mutation

494   rate calculation. After 14 hours, cells were fixed using 2% formaldehyde for 20 minutes. Cells

495   were rinsed with PBS and permeabilized using 0.1% triton-X-100 for 8 minutes. After rinsing

496   again, nonspecific antibody binding sites were blocked using 2% BSA in PBS containing 0.1%

497   tween-20 (PBS-T) for 1 hour. Cells were stained with 1:5000 Hoechst (Life Technologies 33342)

498   and 1:400 anti-GFP Alexa 647 conjugate (Life Technologies A31852) diluted in 2% BSA in PBS-

499   T for 1 hour. After three washes with PBS-T the plates were sealed with black tape prior to

500   removing the final wash. Plates were imaged using an ImageXpress Micro (Molecular

501   Dynamics) using DAPI, Cy5, and FITC specific filter cubes with a 4x magnification lens. The

502   entire surface area of each well was imaged using four non-overlapping quadrants. MetaXpress

503   version 6 software (Molecular Dynamics) was used to count cellular nuclei and antibody stained

504   cells. Cells expressing fluorescent GFP were manually counted from the collected images (11).

505

506   A null class Luria-Delbrück fluctuation test was used to calculate the mutation rates with the

507   equation $\mu_{(s/n/r)} = -\ln(P_0)/(N_f-N_i)$, where $\mu_{(s/n/r)}$ is the mutation rate per strand replicated, P_0 is the

508   proportion of cultures that do not contain a cell infected by a virus encoding fluorescent eGFP,

509   and N_f and N_i are the final and initial viral population sizes, as determined by anti-GFP antibody

510   staining (59, 60). If the number of green cells in a culture was greater than 0.8 (N_f/N_i) it was

511   removed from the calculation because it likely contained a pre-existing fluorescent revertant in

512   the inoculum. Cultures with this many green cells were extremely rare due to the use of a small

513   inoculum (N_i). The null class fluctuation test measurement is most precise when P_0 is between

514   0.1 and 0.7. As a result of lower titers from drug treated viral cultures, not all of our

515   measurements fell within this range. Replicates for which the P_0 was greater than 0.7 are

516   indicated in the mutation rate figures (Figures 3 and 4)

517

518   **Acknowledgments**

20

527

References

529   1.   **Nelson MI**, **Holmes EC**. 2007. The evolution of epidemic influenza. Nat Rev Genet
530   **8**:196–205.

531   2.   **Parvin JD**, **Moscona A**, **Pan WT**, **Leider JM**, **Palese P**. 1986. Measurement of the
532   mutation rates of animal viruses: influenza A virus and poliovirus type 1. J Virol **59**:377–
533   383.

534   3.   **Nobusawa E**, **Sato K**. 2006. Comparison of the mutation rates of human influenza A and
535   B viruses. J Virol **80**:3675–3678.

536   4.   **Suárez-López P**, **Ortín J**. 1994. An estimation of the nucleotide substitution rate at
537   defined positions in the influenza virus haemagglutinin gene. J Gen Virol **75 (Pt 2)**:389–
538   393.

539   5.   **Suárez P**, **Valcárcel J**, **Ortín J**. 1992. Heterogeneity of the mutation rates of influenza A
540   viruses: isolation of mutator mutants. J Virol **66**:2491–2494.

541   6.   **Paules C**, **Subbarao K**. 2017. Influenza. Lancet.

542   7.   **Osterholm MT**, **Kelley NS**, **Sommer A**, **Belongia EA**. 2012. Efficacy and effectiveness
543   of influenza vaccines: a systematic review and meta-analysis. Lancet Infect Dis **12**:36–
544   44.

545   8.   **Steinhauer DA**, **Domingo E**, **Holland JJ**. 1992. Lack of evidence for proofreading
546   mechanisms associated with an RNA virus polymerase. Gene **122**:281–288.

547   9.   **Smith EC**, **Blanc H**, **Vignuzzi M**, **Denison MR**. 2013. Coronaviruses Lacking
548   Exoribonuclease Activity Are Susceptible to Lethal Mutagenesis: Evidence for
549   Proofreading and Potential Therapeutics. PLoS Pathog **9**:e1003565.

550   10.   **Smith EC**, **Sexton NR**, **Denison MR**. 2014. Thinking Outside the Triangle: Replication

551   Fidelity of the Largest RNA Viruses. Annual Review of Virology **1**:111–132.

552 11. **Pauly MD**, **Procario M**, **Lauring AS**. 2017. The mutation rates and mutational bias of
553   influenza A virus. bioRxiv.

554 12. **Sanjuán R**. 2010. Mutational fitness effects in RNA and single-stranded DNA viruses:
555   common patterns revealed by site-directed mutagenesis studies. Philos Trans R Soc
556   Lond, B, Biol Sci **365**:1975–1982.

557 13. **Visher E**, **Whitefield SE**, **McCrone JT**, **Fitzsimmons W**, **Lauring AS**. 2016. The
558   Mutational Robustness of Influenza A Virus. PLoS Pathog **12**:e1005856–25.

559 14. **Anderson JP**, **Daifuku R**, **Loeb LA**. 2004. Viral error catastrophe by mutagenic
560   nucleosides. Annu Rev Microbiol **58**:183–205.

561 15. **Bull JJ**, **Sanjuán R**, **Wilke CO**. 2007. Theory of lethal mutagenesis for viruses. J Virol
562   **81**:2930–2939.

563 16. **Lee CH**, **Gilbertson DL**, **Novella IS**, **Huerta R**, **Domingo E**, **Holland JJ**. 1997. Negative
564   effects of chemical mutagenesis on the adaptive behavior of vesicular stomatitis virus. J
565   Virol **71**:3636–3640.

566 17. **Crotty S**, **Cameron CE**, **Andino R**. 2001. RNA virus error catastrophe: direct molecular
567   test by using ribavirin. Proc Natl Acad Sci USA **98**:6895–6900.

568 18. **Loeb LA**, **Mullins JI**. 2000. Lethal mutagenesis of HIV by mutagenic ribonucleoside
569   analogs. AIDS Res Hum Retroviruses **16**:1–3.

570 19. **Grande-Pérez A**, **Sierra S**, **Castro MG**, **Domingo E**, **Lowenstein PR**. 2002. Molecular
571   indetermination in the transition to error catastrophe: systematic elimination of
572   lymphocytic choriomeningitis virus through mutagenesis does not correlate linearly with
573   large increases in mutant spectrum complexity. Proc Natl Acad Sci USA **99**:12938–
574   12943.

575 20. **Cheung PPH**, **Watson SJ**, **Choy K-T**, **Fun Sia S**, **Wong DDY**, **Poon LLM**, **Kellam P**,
576   **Guan Y**, **Malik Peiris JS**, **Yen H-L**. 2014. Generation and characterization of influenza A
577   viruses with altered polymerase fidelity. Nature Communications **5**:4794.

578 21. **Pauly MD**, **Lauring AS**. 2015. Effective lethal mutagenesis of influenza virus by three
579   nucleoside analogs. J Virol **89**:3584–3597.

580 22. **Baranovich T**, **Wong S-S**, **Armstrong J**, **Marjuki H**, **Webby RJ**, **Webster RG**,
581   **Govorkova EA**. 2013. T-705 (favipiravir) induces lethal mutagenesis in influenza A H1N1
582   viruses in vitro. J Virol **87**:3741–3751.

583 23. **Graham AF**, **Kirk C**. 1965. Effect of 5-fluorouracil on the growth of bacteriophage R17. J
584   Bacteriol **90**:928–935.

585 24. **Furuta Y**, **Takahashi K**, **Kuno-Maekawa M**, **Sangawa H**, **Uehara S**, **Kozaki K**, **Nomura**
586   **N**, **Egawa H**, **Shiraki K**. 2005. Mechanism of action of T-705 against influenza virus.
587   Antimicrob Agents Chemother **49**:981–986.

588 25. **Vanderlinden E**, **Vrancken B**, **Van Houdt J**, **Rajwanshi VK**, **Gillemot S**, **Andrei G**,
589   **Lemey P**, **Naesens L**. 2016. Distinct Effects of T-705 (Favipiravir) and Ribavirin on
590   Influenza Virus Replication and Viral RNA Synthesis. Antimicrob Agents Chemother
591   **60**:6679–6691.

592 26. **Eriksson B**, **Helgstrand E**, **Johansson NG**, **Larsson A**, **Misiorny A**, **Norén JO**,
593   **Philipson L**, **Stenberg K**, **Stening G**, **Stridh S**, **Oberg B**. 1977. Inhibition of influenza
594   virus ribonucleic acid polymerase by ribavirin triphosphate. Antimicrob Agents Chemother
595   **11**:946–951.

596 27. **Pfeiffer JK**, **Kirkegaard K**. 2003. A single mutation in poliovirus RNA-dependent RNA
597   polymerase confers resistance to mutagenic nucleotide analogs via increased fidelity.
598   Proc Natl Acad Sci USA **100**:7289–7294.

599 28. **Vignuzzi M**, **Stone JK**, **Arnold JJ**, **Cameron CE**, **Andino R**. 2006. Quasispecies
600   diversity determines pathogenesis through cooperative interactions in a viral population.
601   Nature **439**:344–348.

602 29. **Coffey LL**, **Beeharry Y**, **Bordería AV**, **Blanc H**, **Vignuzzi M**. 2011. Arbovirus high fidelity
603   variant loses fitness in mosquitoes and mice. Proceedings of the National Academy of
604   Sciences **108**:16038–16043.

605 30. **Zeng J**, **Wang H**, **Xie X**, **Yang D**, **Zhou G**, **Yu L**. 2013. An increased replication fidelity
606   mutant of foot-and-mouth disease virus retains fitness in vitro and virulence in vivo.
607   Antiviral Res **100**:1–7.

608 31. **Zeng J**, **Wang H**, **Xie X**, **Li C**, **Zhou G**, **Yang D**, **Yu L**. 2014. Ribavirin-Resistant Variants
609   of Foot-and-Mouth Disease Virus: the Effect of Restricted Quasispecies Diversity on Viral
610   Virulence. J Virol **88**:4008–4020.

611 32. **Sierra M**, **Airaksinen A**, **González-López C**, **Agudo R**, **Arias A**, **Domingo E**. 2007.
612   Foot-and-mouth disease virus mutant with decreased sensitivity to ribavirin: implications
613   for error catastrophe. J Virol **81**:2012–2024.

614 33. **Agudo R**, **Ferrer-Orta C**, **Arias A**, **la Higuera de I**, **Perales C**, **Pérez-Luque R**,
615   **Verdaguer N**, **Domingo E**. 2010. A multi-step process of viral adaptation to a mutagenic
616   nucleoside analogue by modulation of transition types leads to extinction-escape. PLoS
617   Pathog **6**:e1001072.

618 34. **Perales C**, **Agudo R**, **Domingo E**. 2009. Counteracting quasispecies adaptability:
619   extinction of a ribavirin-resistant virus mutant by an alternative mutagenic treatment.
620   PLoS ONE **4**:e5554.

621 35. **Agudo R**, **la Higuera de I**, **Arias A**, **Grande-Pérez A**, **Domingo E**. 2016. Involvement of
622   a joker mutation in a polymerase-independent lethal mutagenesis escape mechanism.
623   Virology **494**:257–266.

624 36. **Pereira-Gómez M**, **Sanjuán R**. 2014. Delayed lysis confers resistance to the nucleoside
625   analogue 5-fluorouracil and alleviates mutation accumulation in the single-stranded DNA
626   bacteriophage ☐X174. J Virol **88**:5042–5049.

23

627 37. **Elena SF**. 2012. RNA virus genetic robustness: possible causes and some
628   consequences. Curr Opin Virol **2**:525–530.

629 38. **Graci JD**, **Gnädig NF**, **Galarraga JE**, **Castro C**, **Vignuzzi M**, **Cameron CE**. 2012.
630   Mutational robustness of an RNA virus influences sensitivity to lethal mutagenesis. J Virol
631   **86**:2869–2873.

632 39. **Lauring AS**, **Acevedo A**, **Cooper SB**, **Andino R**. 2012. Codon usage determines the
633   mutational robustness, evolutionary capacity, and virulence of an RNA virus. Cell Host
634   and Microbe **12**:623–632.

635 40. **Velthuis Te AJW**, **Fodor E**. 2016. Influenza virus RNA polymerase: insights into the
636   mechanisms of viral RNA synthesis. Nat Rev Micro **14**:479–493.

637 41. **Binh NT**, **Wakai C**, **Kawaguchi A**, **Nagata K**. 2014. Involvement of the N-terminal
638   portion of influenza virus RNA polymerase subunit PB1 in nucleotide recognition.
639   Biochem Biophys Res Commun **443**:975–979.

640 42. **Binh NT**, **Wakai C**, **Kawaguchi A**, **Nagata K**. 2013. The N-terminal region of influenza
641   virus polymerase PB1 adjacent to the PA binding site is involved in replication but not
642   transcription of the viral genome. Front Microbiol **4**:398.

643 43. **Naito T**, **Mori K**, **Ushirogawa H**, **Takizawa N**, **Nobusawa E**, **Odagiri T**, **Tashiro M**,
644   **Ohniwa RL**, **Nagata K**, **Saito M**. 2017. Generation of a Genetically Stable High-Fidelity
645   Influenza Vaccine Strain. J Virol **91**:e01073–16.

646 44. **Velthuis Te AJW**, **Fodor E**. 2016. Influenza virus RNA polymerase: insights into the
647   mechanisms of viral RNA synthesis. Nat Rev Micro **14**:479–493.

648 45. **Pflug A**, **Guilligay D**, **Reich S**, **Cusack S**. 2014. Structure of influenza A polymerase
649   bound to the viral RNA promoter. Nature **516**:355–360.

650 46. **Reich S**, **Guilligay D**, **Pflug A**, **Malet H**, **Berger I**, **Crépin T**, **Hart D**, **Lunardi T**, **Nanao
651   M**, **Ruigrok RWH**, **Cusack S**. 2014. Structural insight into cap-snatching and RNA
652   synthesis by influenza polymerase. Nature **516**:361–366.

653 47. **Arnold JJ**, **Vignuzzi M**, **Stone JK**, **Andino R**, **Cameron CE**. 2005. Remote site control
654   of an active site fidelity checkpoint in a viral RNA-dependent RNA polymerase. J Biol
655   Chem **280**:25706–25716.

656 48. **Korneeva VS**, **Cameron CE**. 2007. Structure-function relationships of the viral RNA-
657   dependent RNA polymerase: fidelity, replication speed, and initiation mechanism
658   determined by a residue in the ribose-binding pocket. J Biol Chem **282**:16135–16145.

659 49. **Campagnola G**, **McDonald S**, **Beaucourt S**, **Vignuzzi M**, **Peersen OB**. 2014. Structure-
660   Function Relationships Underlying the Replication Fidelity of Viral RNA-Dependent RNA
661   Polymerases. J Virol **89**:275–286.

662 50. **Arias A**, **Arnold JJ**, **Sierra M**, **Smidansky ED**, **Domingo E**, **Cameron CE**. 2008.
663   Determinants of RNA-dependent RNA polymerase (in)fidelity revealed by kinetic analysis
664   of the polymerase encoded by a foot-and-mouth disease virus mutant with reduced

24

665   sensitivity to ribavirin. J Virol **82**:12346–12355.

666   51.   **Lauring AS**, **Frydman J**, **Andino R**. 2013. The role of mutational robustness in RNA
667   virus evolution. Nat Rev Micro **11**:327–336.

668   52.   **Marsh GA**, **Hatami R**, **Palese P**. 2007. Specific residues of the influenza A virus
669   hemagglutinin viral RNA are important for efficient packaging into budding virions. J Virol
670   **81**:9727–9736.

671   53.   **Baker SF**, **Nogales A**, **Finch C**, **Tuffy KM**, **Domm W**, **Perez DR**, **Topham DJ**, **Martínez-**
672   **Sobrido L**. 2014. Influenza A and B Virus Intertypic Reassortment through Compatible
673   Viral Packaging Signals. J Virol **88**:10778–10791.

674   54.   **Hoffmann E**, **Neumann G**, **Kawaoka Y**, **Hobom G**, **Webster RG**. 2000. A DNA
675   transfection system for generation of influenza A virus from eight plasmids. Proc Natl
676   Acad Sci USA **97**:6108–6113.

677   55.   **Hoffmann E**, **Stech J**, **Guan Y**, **Webster RG**, **Perez DR**. 2001. Universal primer set for
678   the full-length amplification of all influenza A viruses. Arch Virol **146**:2275–2289.

679   56.   **Ho SN**, **Hunt HD**, **Horton RM**, **Pullen JK**, **Pease LR**. 1989. Site-directed mutagenesis by
680   overlap extension using the polymerase chain reaction. Gene **77**:51–59.

681   57.   **Martínez-Sobrido L**, **Cadagan R**, **Steel J**, **Basler CF**, **Palese P**, **Moran TM**, **García-**
682   **Sastre A**. 2010. Hemagglutinin-pseudotyped green fluorescent protein-expressing
683   influenza viruses for the detection of influenza virus neutralizing antibodies. J Virol
684   **84**:2157–2163.

685   58.   **REED LJ**, **MUENCH H**. 1938. A SIMPLE METHOD OF ESTIMATING FIFTY PER CENT
686   ENDPOINTS, **27**:493–497.

687   59.   **Furió V**, **Moya A**, **Sanjuán R**. 2005. The cost of replication fidelity in an RNA virus. Proc
688   Natl Acad Sci USA **102**:10233–10237.

689   60.   **Foster PL**. 2006. Methods for determining spontaneous mutation rates. Meth Enzymol
690   **409**:195–213.

691

692

693 **Figure Legends**

694 Figure 1. Sensitivity of influenza polymerase mutants to nucleoside analogs. MDCK cells were

695 pretreated with media containing 0μM drug, 100μM 5-fluorouracil, 20μM ribavirin, or 20μM 5-

696 azacytidine for 3 hours and then infected with virus at an MOI of 0.1. After 24 hours, cell free

697 supernatants were harvested and titered by $TCID_{50}$. The decrease in the log of the infectious

698 titer for drug-treated samples relative to untreated samples for each virus is shown. Three

699 replicate samples were harvested for each virus at each drug concentration and are shown

700 along with the mean. The statistical significance of the decrease in the base 10 logarithmic titer

701 of each mutant relative to WT PR8 was determined by one-way ANOVA with a Dunnett's

702 multiple comparison test. * = p-value < 0.05, ** = p-value < 0.001.

703

704 Figure 2. Replicative fitness of influenza polymerase mutants. (A) Direct competition assays

705 were performed for each mutant against a WT PR8 virus containing a neutral genetic barcode.

706 For each competition, a 1:1 starting mixture of each virus (by infectious titer) was passaged four

707 times on MDCK cells at an MOI of 0.01. The relative changes in the amounts of the two

708 competing viruses were determined by quantitative RT-PCR. Relative fitness was calculated as

709 described in Methods. Data are shown for three individual competitions along with the mean.

710 The statistical significance of the fitness values for each mutant relative to WT PR8 was

711 determined by one-way ANOVA with a Dunnett's multiple comparison test. * = p-value < 0.05, **

712 = p-value < 0.01, *** = p-value < 0.001. (B) MDCK cells were infected at an MOI of 0.1 and

713 quantitative RT-PCR was used to measure the genome copy number. The data were analyzed

714 using a two-way ANOVA and mutant viruses were compared with the WT using Sidak's multiple

715 comparison test. (C) Competition assays were performed as above for the PB1 T123A, PA T97I,

716 and the PB1 T123A, PA T97I mutant in the presence of 5-fluorouracil. For each virus, a one-

26

717   way ANOVA with a Dunnett's multiple comparison test was used to compare the relative fitness

718   of drug treated virus to non-treated virus. * = p-value < 0.05, ** = p-value < 0.01, *** = p-value <

719   0.001

720

721   Figure 3. Mutation rates of influenza polymerase mutants. Rates of the four transition mutation

722   classes were measured using a 12-class fluctuation test. Data points are color coded by virus.

723   Measurements within the ideal P_0 range of 0.1 - 0.7 for the null class method are shown as filled

724   symbols. Those outside of that range, with P_0 values between 0.7 – 0.9, are shown as open

725   symbols. Arithmetic means are shown for the replicate measurements. The statistical

726   significance of the differences in mutation rates for each mutation class of each mutant relative

727   to WT PR8 was determined by one-way ANOVA with Dunnett's multiple comparison test. * = p-

728   value < 0.05, ** = p-value < 0.01.

729

730   Figure 4. Effect of 5-fluoruracil on viral mutation rate. Mutation rates were measured as in

731   Figure 3 using a 12-class fluctuation test. The rates of four mutation classes; A to G, C to U, G

732   to A, and U to C, were measured in the presence of 15μM 5-fluorouracil for the indicated viruses.

733   For each virus and mutational class, the statistical significance of the difference in mutation

734   rates in the presence and absence of 5-fluorouracil was determined using t-tests and the Holm-

735   Sidak correction for multiple comparisons. * = p-value < 0.05, ns = not significant.

736

737   Figure 5. The effect of 5-fluorouracil on the specific infectivity. MDCK cells were treated with or

738   without 100μM 5-fluorouracil and infected with influenza at an MOI of 0.1 for 24 hours. For each

739   sample, the infectious titer was measured by $TCID_{50}$, and the genome copy number was

740   measured by quantitative RT-PCR. The specific infectivity was calculated as the titer divided by

741   the genome copy number. The decreases in the $\log_{10}$ of the specific infectivity for 100μM 5-

742   fluorouracil treated samples relative to non-treated samples are shown for replicate

743   measurements from two or three individual experiments. There were no statistically significant

744   differences when the data were analyzed using a one-way ANOVA.

745

746   Figure 6. Genome production by influenza mutants during 5FU treatment. MDCK cells were

747   infected with wild type, PB1 T123A, PA T97I, or PB1 T123A ; PA T97I viruses at an MOI of 0.1

748   in either 0μM (solid lines) or 100μM 5-fluorouracil (dashed lines). Supernatants were collected

749   at four hour intervals. The number of M genome segment copies per mL was determined by

750   quantitative RT-PCR. Data are mean ± standard deviation for 3 replicates ($\log_{10}$ scale).

751   Genome production over time was compared in the presence and absence of drug for each

752   virus using a two-way ANOVA with a Sidak multiple comparison test. * = p-value < 0.05, ** = p-

753   value < 0.01, *** = p-value < 0.001, **** = p-value < 0.0001.

754

28

Figure 1

Figure 1. Sensitivity of influenza polymerase mutants to nucleoside analogs. MDCK cells were pretreated with media containing 0μM drug, 100μM 5-fluorouracil, 20μM ribavirin, or 20μM 5-azacytidine for 3 hours and then infected with virus at an MOI of 0.1. After 24 hours, cell free supernatants were harvested and titered by TCID50. The decrease in the log of the infectious titer for drug-treated samples relative to untreated samples for each virus is shown. Three replicate samples were harvested for each virus at each drug concentration and are shown along with the mean. The statistical significance of the decrease in the base 10 logarithmic titer of each mutant relative to WT PR8 was determined by one-way ANOVA with a Dunnett's multiple comparison test. * = p-value < 0.05, ** = p-value < 0.001.

Figure 2
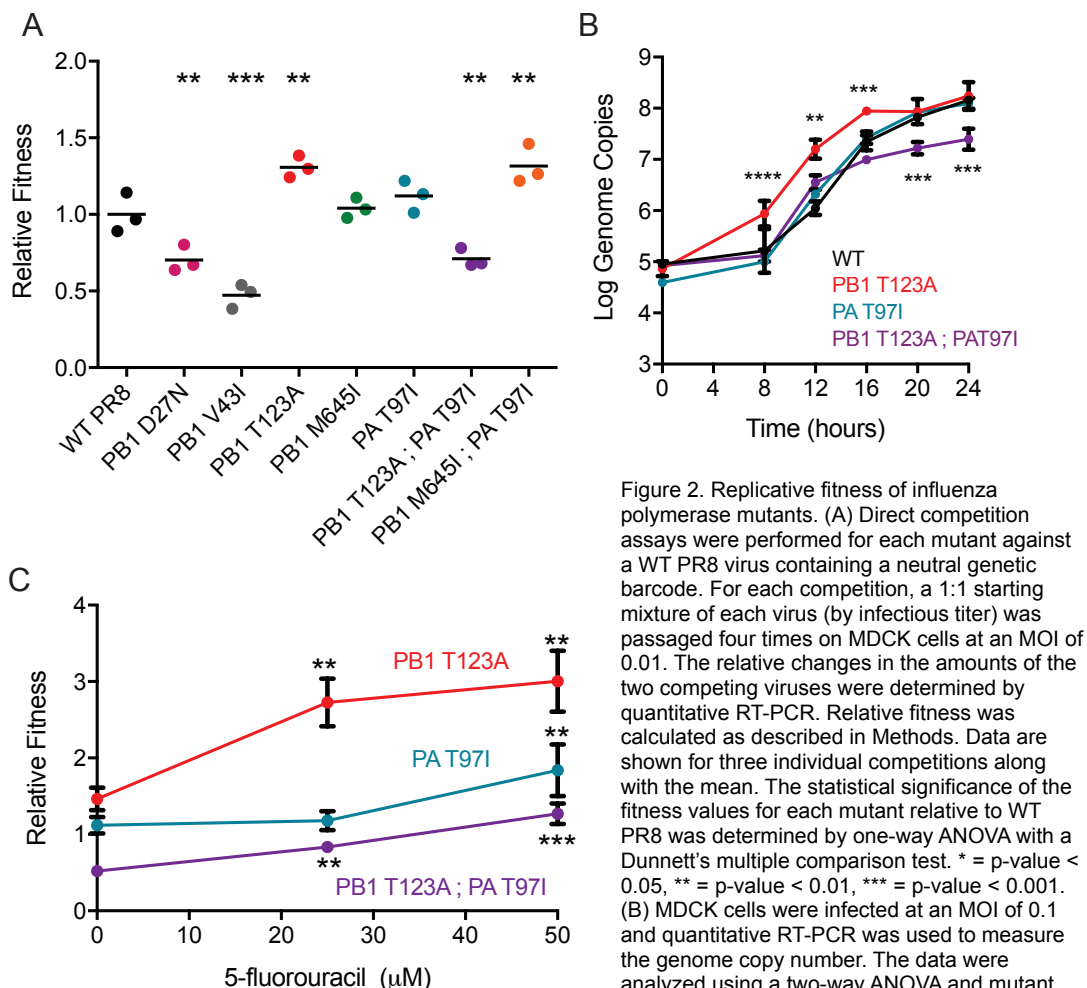
Figure 2. Replicative fitness of influenza polymerase mutants. (A) Direct competition assays were performed for each mutant against a WT PR8 virus containing a neutral genetic barcode. For each competition, a 1:1 starting mixture of each virus (by infectious titer) was passaged four times on MDCK cells at an MOI of 0.01. The relative changes in the amounts of the two competing viruses were determined by quantitative RT-PCR. Relative fitness was calculated as described in Methods. Data are shown for three individual competitions along with the mean. The statistical significance of the fitness values for each mutant relative to WT PR8 was determined by one-way ANOVA with a Dunnett's multiple comparison test. * = p-value < 0.05, ** = p-value < 0.01, *** = p-value < 0.001. (B) MDCK cells were infected at an MOI of 0.1 and quantitative RT-PCR was used to measure the genome copy number. The data were analyzed using a two-way ANOVA and mutant viruses were compared with the WT using Sidak's multiple comparison test. (C) Competition assays were performed as above for the PB1 T123A, PA T97I, and the PB1 T123A, PA T97I mutant in the presence of 5-fluorouracil. For each virus, a one-way ANOVA with a Dunnett's multiple comparison test was used to compare the relative fitness of drug treated virus to non-treated virus. * = p-value < 0.05, ** = p-value < 0.01, *** = p-value < 0.001
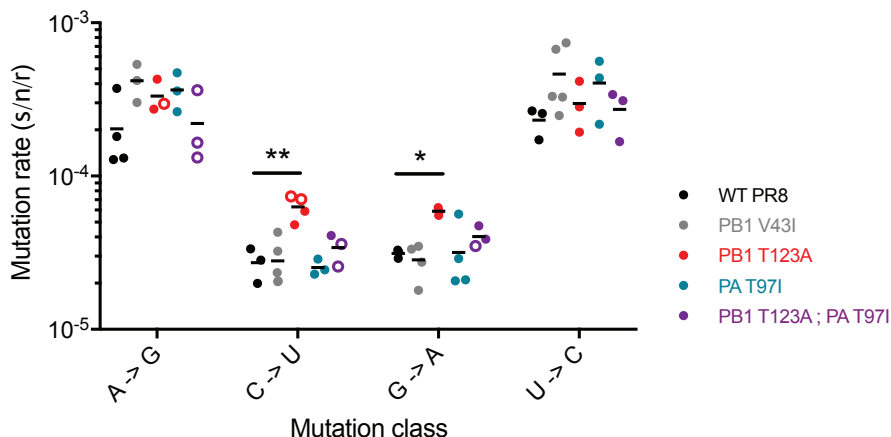
Figure 3

Figure 3. Mutation rates of influenza polymerase mutants. Rates of the four transition mutation classes were measured using a 12-class fluctuation test. Data points are color coded by virus. Measurements within the ideal P0 range of 0.1 - 0.7 for the null class method are shown as filled symbols. Those outside of that range, with P0 values between 0.7 – 0.9, are shown as open symbols. Arithmetic means are shown for the replicate measurements. The statistical significance of the differences in mutation rates for each mutation class of each mutant relative to WT PR8 was determined by one-way ANOVA with Dunnett's multiple comparison test. * = p-value < 0.05, ** = p-value < 0.01.
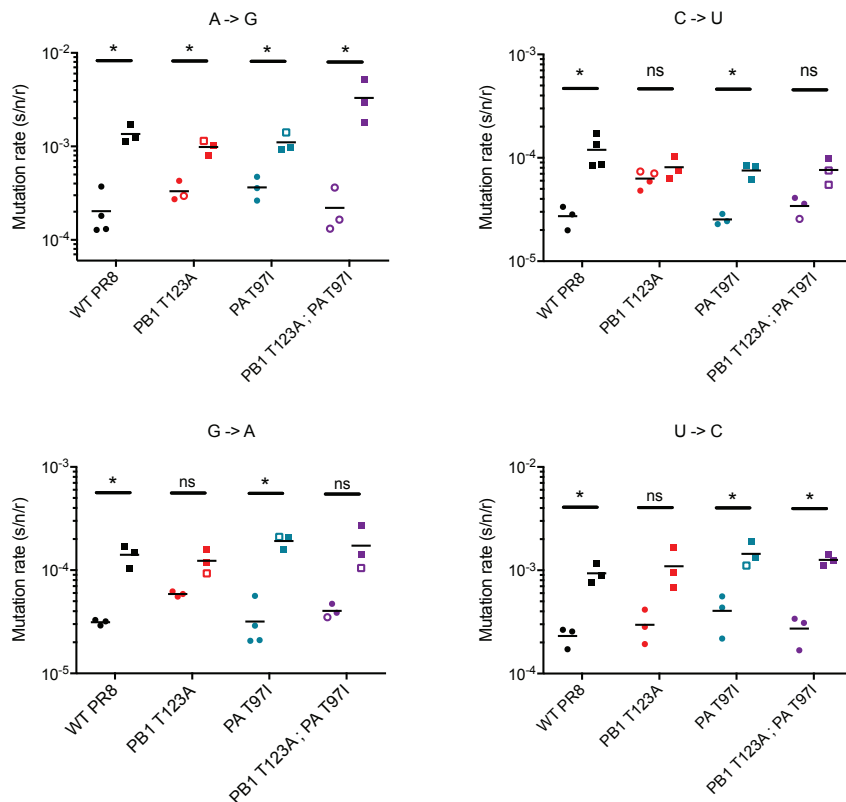
Figure 4

Figure 4. Effect of 5-fluoruracil on viral mutation rate. Mutation rates were measured as in Figure 3 using a 12-class fluctuation test. The rates of four mutation classes; A to G, C to U, G to A, and U to C, were measured in the presence of 15μM 5-fluorouracil for the indicated viruses. For each virus and mutational class, the statistical significance of the difference in mutation rates in the presence and absence of 5-fluorouracil was determined using t-tests and the Holm-Sidak correction for multiple comparisons. * = p-value < 0.01, ns = not significant, p <0.05.
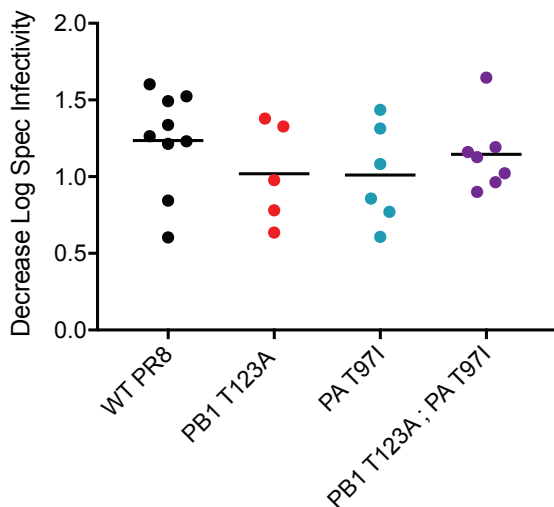
Figure 5

Figure 5. The effect of 5-fluoruracil on the specific infectivity. MDCK cells were treated with or without 100µM 5-fluorouracil and infected with influenza at an MOI of 0.1 for 24 hours. For each sample, the infectious titer was measured by TCID50, and the genome copy number was measured by quantitative RT-PCR. The specific infectivity was calculated as the titer divided by the genome copy number. The decreases in the log10 of the specific infectivity for 100µM 5-fluorouracil treated samples relative to non-treated samples are shown for replicate measurements from two or three individual experiments. There were no statistically significant differences when the data were analyzed using a one-way ANOVA.
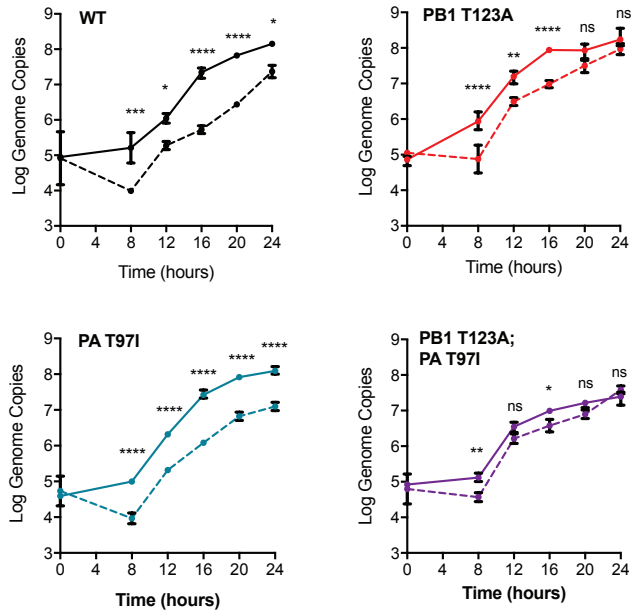
Figure 6

Figure 6. Genome production by influenza mutants during 5FU treatment. MDCK cells were infected with wild type, PB1 T123A, PA T97I, or PB1 T123A ; PA T97I viruses at an MOI of 0.1 in either 0μM (solid lines) or 100μM 5-fluorouracil (dashed lines). Supernatants were collected at four hour intervals. The number of M genome segment copies per mL was determined by quantitative RT-PCR. Data are mean ± standard deviation for 3 replicates (Log10 scale). Genome production over time was compared in the presence and absence of drug for each virus using a two-way ANOVA with a Sidak multiple comparison test. * = p-value < 0.05, ** = p-value < 0.01, *** = p-value < 0.001, **** = p-value < 0.0001.